

Enhancing performance for three-phase induction motor by changing the magnetic flux density and core material using COMSOL

Firas Saaduldeen Ahmed¹, Zozan Saadallah Hussain¹, Truska Khalid Mohammed Salih²

¹Department of Electrical Techniques, Technical Institute of Mosul, Northern Technical University, Mosul, Iraq

²Department of Electricity, Erbil Technology Collage, Erbil Polytechnic University, Erbil, Iraq

Article Info

Article history:

Received Apr 27, 2021

Revised Jun 28, 2021

Accepted Jul 9, 2021

Keywords:

Aluminum

Cast iron

Finite element method

Frequency domain

Magnetic flux density

ABSTRACT

This paper presents a proposed design and analysis of a three-phase squirrel cage induction motor when changing of internal characteristic design for the three-phase induction motor. Two situations have been applied to enhancing the performance of the three-phase induction motor. The first situation has been implemented by changing the magnetic flux density (MFD) via the build of the six-phase for the same induction motor. The second situation has been implemented by changing core materials of the rotor part of the induction motor, like aluminum (AL) and cast iron (CI). The finite element method (FEM) has been used to analyze the rotor part, also to obtain the representation and simulation of the realty cylindrical rotor part of motor. The frequency domain (FD) analysis using to obtain the results within the environment of the COMSOL multiphysics 5.5 version.

This is an open access article under the [CC BY-SA](https://creativecommons.org/licenses/by-sa/4.0/) license.



Corresponding Author:

Firas Saaduldeen Ahmed

Department of Electrical Techniques, Technical Institute of Mosul, Northern Technical University

Mosul, Iraq

Email: firas_saad@ntu.edu.iq

1. INTRODUCTION

Induction motors (or asynchronous motors) now account for about half of total electricity use in industrialized countries. Furthermore, A.C. motors consume a significant amount of power in the agricultural and industrial sectors. The quantity of energy consumed by a motor over its life cycle is calculated to be 60-100 times the motor's initial cost [1]. Technological characteristics enjoyed by this type of induction motors squirrel cage, such as low maintenance cost, high reliability, high performance, and a good starting torque. Also, the type of rotor has the easy and most rugged construction imaginable and is nearly indestructible. Therefore, squirrel cage induction motor is one of the most versatile electric machines of previously and today, where being form in approximately 70% of global industry and also consuming around 50% of the energy generated on the planet and other applications about machines [2], [3].

The induction motor has consisted of a laminated stator and rotor core. The classic design induction motor stator has one set of 3-phase windings that are spatially distributed uniformly around the stator and is driven by a sinusoidal balanced polyphase excitation that drives currents through the stator windings, in which symmetrical three-phase voltages displaced by 120 (electrically) are supplied [2]. While the stator of a 6-ph of induction motor (I.M) comprises two groups for different 3-ph windings that are offset by a particular angle from one another. It has axial rotor bars that are often cast in aluminum or copper [4]. Electric current passes through the stator conductors, producing a magnetic field that rotates at a synchronous speed. The single cage rotor is the most common rotor bar type. Single layer windings have been used in small (AC)

motors, and a single-layer winding is an example of a three-phase concentric winding [5]. Mathematical models have been created and analyzed by two concept three-phase and six-phase induction motor [6]. The criteria for selecting the starting points for each phase were proposed as a general formula for determining the number of slots available for an N-phase alternating current machine design [7]. In industrial drives, six-phase induction motors have numerous benefits over traditional 3-phase motors including reduced magnetic flux harmonics, increased stability, reduces torque pulsations, and lower power levels for the static converter [8]. It is important to establish models for these phenomena to gain a deeper understanding of them. The numerical electromagnetic field measurement is good method for designing and calculating induction motors or electrical machines. Other researchers proposed a method to describe a 3-ph linear I.M to determine the different values employed in its /phase duplicate circuit by a DSP system [9]. It has found that the air gap in linear induction motors (LIMs) is much larger than in rotary induction motors (RIMs). The secondary parameters have determined using two methods based on MATLAB-Simulink [10].

For analyses of electrical machines, the finite element method (FEM) uses the subdivision of a large problem domain into more simple sections called finite elements and variational methods to solve the problem by reducing a related error function [11]-[13]. MATLAB simulation based on the symmetrical component theory, the estimated performance of a three-phase IM at steady-state, such as under/over and unbalanced/balanced voltage disturbances at different values of VUF, has been analyzed [14], [15]. The T-slip characteristics and S.state power losses have also been measured and plotted at various degrees of voltage unbalance. The modern programs help design the electrical machines on the reducing cost of the application and which lead to achieving the best results for the design before building real the structure of the machines [14].

COMSOL multiphysics is one of the most successful simulation programs used in design the induction motor and it's used in other applications [16]. It has been used in this current work to analyze induction motor parameters. The "rotating machinery" interface in COMSOL multiphysics 5.5 has used to run a frequency domain and non-linear simulation of an induction machine's dynamic activity action. The two-dimensional FEM model is linked to electrical circuits by connecting the physics interfaces "rotating machinery" and "electrical circuit" [17]. Also, the COMSOL multiphysics has included the multi-time analysis in the same program like time-dependent, frequency-domain [18]. The two-dimensional model in the COMSOL program is a perfect method for studying induction motor behavior under different situations, speed, torque, and current values are depending on the precision of identification and calculation of induction motor parameters, geometry, and material properties [19].

FE program, traditional analysis calculation, and actual measurement have been used to look into the flux density in the air gap, torque output of the dual 3-ph motor [18]. Trapezoidal wave phase current has used by investigating the air-gap field density of a 6-phase induction motor [20]. The induction motor has represented as a two-dimensional model with specified out-of-plane thickness. As a quasi-3D model. The COMSOL AC/DC module's rotating machinery, the magnetic interface is used for stationery and time-domain modeling [21], [22]. The dependent variables in this physical interface, which satisfies Maxwell's equations, are the magnetic vector potential and magnetic scalar potential [21]. The magnetic interface of the nodes ampere's law has used in the rotating machinery to solve the magnetic field in the motor [23]-[25]. The main problem of the 3-phase induction motor is the beginning of the start operation torque and distribution of magnetic flux density. Therefore, this present paper suggested enhancing the performance design of a 3-phase induction motor squirrel cage by COMSOL multiphysics.

The contribution of this work to the first time has used the flux density results and change of the core material in the same design by COMSOL software program. In this paper has been changed the magnetic flux density (MFD) for the three-phase and six phases of the squirrel cage induction motor and compares the two cases above. In addition, two materials have used frequency-domain analysis in the design of a six-phase induction motor. The first material is aluminum (AL), and the second cast iron (CI) material. These materials have applied to the rotor part of the motor on six phases of induction motor to obtain the best results. FEM has been used to analyze the result of torque (N/m) with omega speed (rad/s) to know which material is better than the design of the six phases in the induction motor. The values of the parameter of the electrical conductivity, relative permeability, and relative permittivity have taken from the default of the same program (add materials) of the COMSOL.

2. RESEARCH METHOD

A 3-phase induction motor's performance can be improved by modifying the MFD and the core materials of the rotor part. This design requires high accuracy for the same parameters of the motor to keep the comparison between three and six phases of design.

2.1. Induction motor construction

The induction motor is made up of two parts:

- a) The stator, which is the outer component
- b) The rotating component

The stator and rotor are both constructed of:

- a) The electric circuit, which is often built of insulated aluminum or copper winding, carries current
- b) The magnetic circuit, which is typically constructed from a series of laminated silicon steel laminations pressed together to produce a cylindrical magnetic circuit to carry MFD current

There are many important equations to consider when designing an induction motor stator [26]-[31]. For full pitch, pitch factor ($K_p = 1$). The motor output power (P_{out}) is calculated as in (1):

$$P_{out} = HP \times 746 \quad (1)$$

where (HP) stands for horse power in a motor. The input apparent power (KVA_i) of a motor can be determined as in (2):

$$KVA_i = \frac{P_{out}}{\eta \times pf} \quad (2)$$

where (η), (pf) are a motor's efficiency and power factor respectively. The synchronous speed of the motor in revolutions per second (N_{ss}) can be calculated as in (3):

$$N_{ss} = \frac{f}{P/2} \quad (3)$$

where (f) is the frequency of supply. The output coefficient (C_o) is calculated as (4):

$$C_o = 1.11\pi^2 B_{av} ac K_w 10^{-3} \quad (4)$$

where B_{av} represents the average flux density and is the ampere conductor per meter. The stator's diameter and length are as in (5)-(8).

$$DSi^2 L = \frac{KVA_i}{C_o \times N_{ss}} \quad (5)$$

$$DSi^3 = \frac{DSi^2 L \times P}{\pi \times L/\tau} \quad (6)$$

$$DSi = \sqrt[3]{DSi^3} \quad (7)$$

$$L = \frac{DSi^2 L}{DSi^2} \quad (8)$$

where:

DSi = the stator's inner diameter,

L = length, and

τ = pole pitch.

The magnetic flux (\emptyset) can be determined as (9).

$$\emptyset = \frac{B_{av} \times \pi \times DSi \times L}{P} \quad (9)$$

The number of turns per phase (T_{ph}) is calculated as (10):

$$T_{ph} = \frac{V_{ph}}{4.44 \times K_w \times f \times \emptyset} \quad (10)$$

where (V_{ph}) is the voltage per phase. The total number of conductors (Z_t) is calculated as in (11):

$$Z_t = 2 \times n \times T_{ph} \quad (11)$$

where (n) denotes the total number of phases. The number of conductors per stator slot (ZS_s) is as (12).

$$ZS_s = \frac{Z_t}{S_s} \quad (12)$$

The current density (J) is measured as in (13):

$$J = \frac{I_{ph}}{A_{cu}} \quad (13)$$

where (A_{cu}) is the area of one conductor. And the rated per phase current (I_{ph}) is calculated as in (14).

$$I_{ph} = \frac{KVA_i}{n \times V_{ph}} \quad (14)$$

The area of conductors per stator slot (AS_c) equals:

$$AS_c = ZS_s \times A_{cu} \quad (15)$$

and the area of the stator slot (AS_s) is calculated as in (16):

$$AS_s = \frac{AS_c}{1 - spf} \quad (16)$$

where: (spf) denotes the space factor. The diameter of one stator slot (DS_s) is given by (17).

$$DS_s = 2 \times \sqrt{\frac{AS_s}{\pi}} \quad (17)$$

The stator's outer diameter (DS_o) is calculated as in (18).

$$DS_o = DS_i + 2 \times (2 \times DS_s) \quad (18)$$

The air gap length (Lg_1) is calculated as in (19),

$$Lg_1 = 0.2 + 2 \times \sqrt{DS_i \times L} \quad (19)$$

and the rotor's outer diameter (DR_o) is determined as in (20).

$$DR_o = DS_i - 2 \times Lg_1 \quad (20)$$

2.2. Induction motor with three phases

The following equations would apply to 3-phase induction motors. The quantity of slits/pole every phase (S_{spp}) is determined as in (21):

$$S_{spp} = \frac{S_s}{3 \times P} \quad (21)$$

where (P) is the number of stator slots and is the number of poles. The slot electrical angle (α_e) is calculated as in (22).

$$\alpha_e = \frac{180 \times P}{S_s} \quad (22)$$

Furthermore, the distribution factor (K_d) equals:

$$K_d = \frac{\sin\left(S_{spp} \times \frac{\alpha_e}{2}\right)}{S_{spp} \times \sin\frac{\alpha_e}{2}} \quad (23)$$

The winding factor (K_w) was calculated as in (24).

$$K_w = K_p \times K_d \quad (24)$$

The total number of conductors (Z_t) is calculated as in (25).

$$Z_t = 2 \times 3 \times T_{ph} \quad (25)$$

The rated per phase current (I_{ph}) is determined as in (26).

$$I_{ph} = \frac{KVA_i}{3 \times V_{ph}} \quad (26)$$

2.3. Induction motor with six phases

A 6-phase induction motor has a different stator than a 3-ph induction motor. The following are the equations for a 6-ph induction motor. The quantity of slits/poles per phase (S_{spp}) determined as (27).

$$S_{spp} = \frac{S_s}{6 \times P} \quad (27)$$

While the distribution factor is one for a six phase, four pole, twenty-four slot stator, the (S_{spp}) is one.

$$K_d = 1, \text{ and } K_w = 1$$

The total number of conductors (Z_t) is calculated as in (28).

$$Z_t = 2 \times 6 \times T_{ph} \quad (28)$$

The rated per phase current (I_{ph}) is determined as in (29).

$$I_{ph} = \frac{KVA_i}{6 \times V_{ph}} \quad (29)$$

The main dimensions of model geometry are two-dimensional and is depicted in Figure 1.

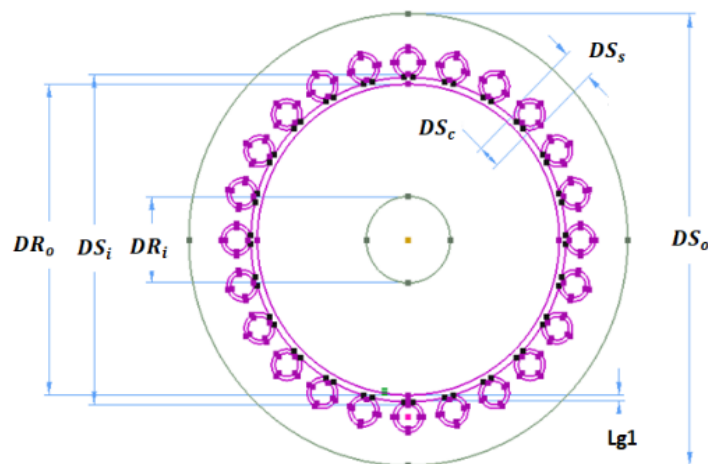


Figure 1. Depicts the dimensions of an induction motor

2.4. Result of stator design

The following are the requirements for the induction motor to be designed: 2 horse power (HP), 4 pole (P), supply frequency of 50 hertz (f), supply voltage 400 volt (VL), efficiency of 80% (η), full pitch, 0.825 full load power factor (pf), unity ratio of pole length to pole pitch (L/τ), 0.25 space factor (spf), 24 stator slots (Ss), average flux density (B_{av}) of 0.44 Wb/m², electrical loading (ac) of 18000 ac/m.

A 20 SWG enameled copper coil, Dc (conductor diameter) = 0.914 mm, and Acu = 0.656118 mm² conductor area are used for three phase winding. Table 1 displays the outcome of designing the stator of a 3-phase IM. A 22 SWG enameled copper coil, diameter of the conductor (Dc) = 0.711 mm, and area of the conductor (Acu) = 0.397035265 mm² are used for the six-phase winding. Table 2 shows the outcome of designing the stator of a 6-phase IM.

Table 1. Design details for a two-horsepower 3-phase induction motor stator

Parameter	Value	Unit
DSo	157	Millimeters
DSi	112.6879193	Millimeters
DSs	10.83174626	Millimeters
DSc	8.123809697	Millimeters
DRo	112.0879193	Millimeters
Tph	316	Turns
Iph	3.262903794	Ampere
J	4.9730405	A/mm ²
ZSs	79	Conductor
Lg1	0.3	Millimeters

Table 2. Design details for a two-horsepower stator for a 6-phase induction motor

Parameter	Value	Unit
DSo	159	Millimeters
DSi	111.3931845	Millimeters
DSs	11.80250482	Millimeters
DSc	8.851878614	Millimeters
DRo	110.7931845	Millimeters
Tph	310	Turns
Iph	1.631451897	Ampere
J	4.109085618	A/mm ²
ZSs	155	Conductor
Lg1	0.3	Millimeters

The per-phase current in a six-phase stator is half that of a three-phase stator; with a lower current. A smaller cross-section area for wire has used, so the normal wire gauge has been modified from 20 to 22, and the current density in the six-phase windings is around 82 percent of the three-phase windings, a ratio of current density as in (30).

$$\text{Current density ratio} = \frac{J_{\text{six-phase}}}{J_{\text{three-phase}}} = 0.83 \quad (30)$$

The number of turns and conductors measured as an integer number. After rounding, the number of turns for each phase of the 3-phase motor is 316 turns, while for each phase of the six-phase motor is 310 turns; this small difference is primarily due to the winding factor. As shown in the preceding tables, the number of conductors per slot varies greatly, with 79 conductors per slot for three-phase stators and 155 conductors per slot for six-phase stators. However, since the cross-section area of 22 SWG wire is less than that of 20 SWG wire, the number of conductors per slot ratio is as in (31).

$$\text{Conductor per slot ratio} = \frac{ZS_{\text{six-phase}}}{ZS_{\text{three-phase}}} = 1.96 \quad (31)$$

3. SIMULATION RESULTS

The design of induction motor has been simulation by COMSOL multiphysics 5.5. The design has taken to compare between the three and six phases to know how the performance-enhancing by two simulation results, first the distribution of flux density to it, and the second changing of the core materials in

the FD to know the relation between torque and speed. Figure 2 shows the distribution of MFD in the 3ph induction motor design. Figure 4 shows the distribution of MFD of three-phase induction motor when it has taken the effect of rotor part rotational considered. Also, it observed the weak flux density on the distribution of rotor part, and the directional of rotation is anti-clockwise. Figure 5 shows the distribution of MFD of six-phase induction motor when it has taken the effect of rotor part rotational considered. Also, it observed the regularity flux density on the distribution of rotor part, more uniform intensity, and the directional of rotation is anti-clockwise.

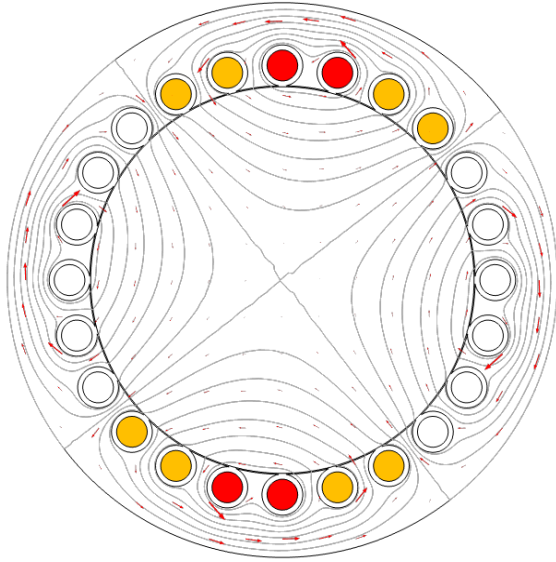


Figure 2. Three-phase MFD distribution in induction motor

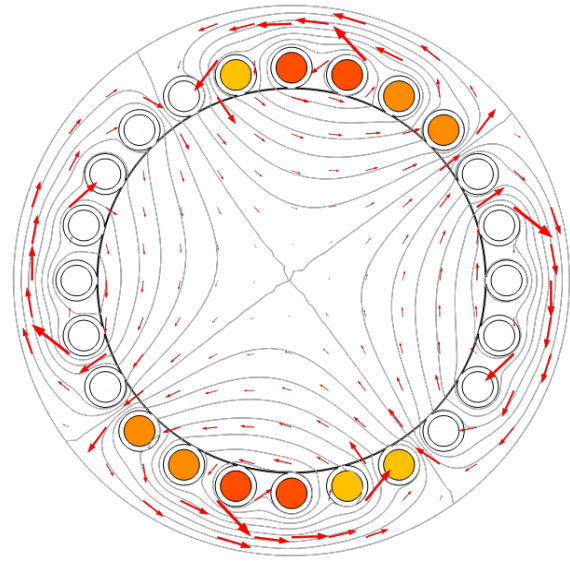


Figure 3. Six-phase MFD distribution in induction motor

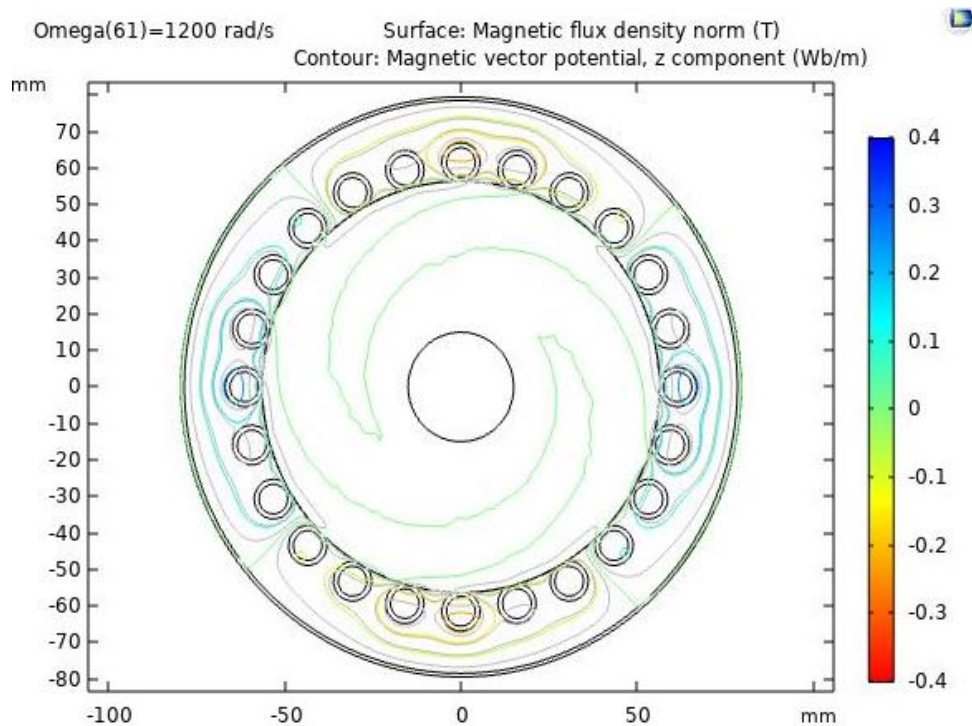


Figure 4. Distribution of MFD in the rotor part for three-phase induction motor when FEM has taken considered

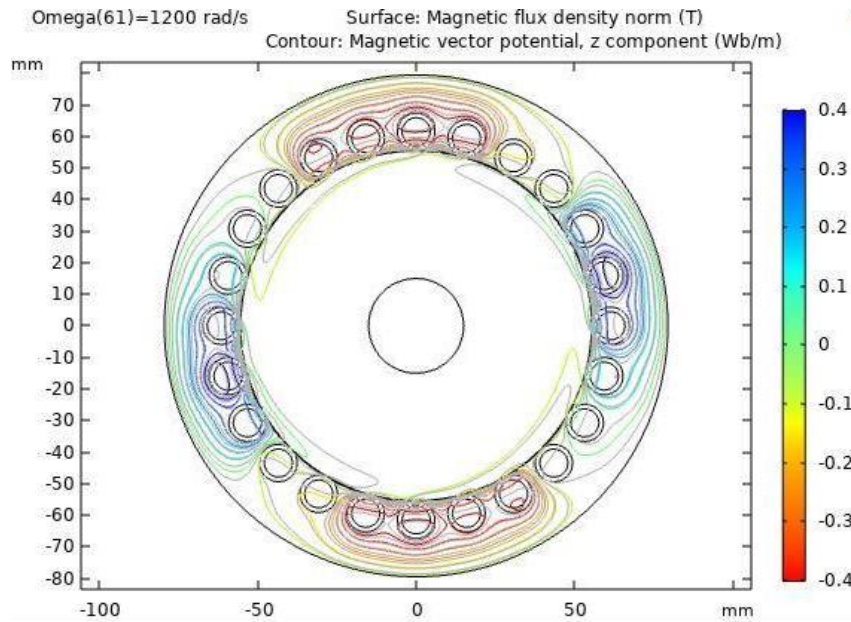


Figure 5. Distribution of MFD in the rotor part for six-phase induction motor when FEM has taken considered

Figure 6 shows the mesh configuration established of the six-phase induction motor in the air gap way with free triangles, and the color blue is shown slots of conductor winding in the stator part. Figure 7 shows the relation between torque (N*m) and angular velocity Omega (rad/s) when has been chosen the frequency domain analysis in a 3-ph induction motor. Also, it detected the starting torque beginning and ending in the negative value. Because the field strength is low and, therefore the torque is small and starts with a negative value. It is worth mentioning the AL core material is employed in the rotor part of the 3-phase induction motor because it does not show different results when the materials are changing.

Figure 8 shows the relation between torque (N*m) and angular velocity Omega (rad/s) when has been chosen the frequency domain analysis in a six-phase induction motor. Also, it observed the starting torque beginning is positive because of the increase in the flux density and ending in the negative value at the steady-state. The material has used in the rotor part is aluminum material.

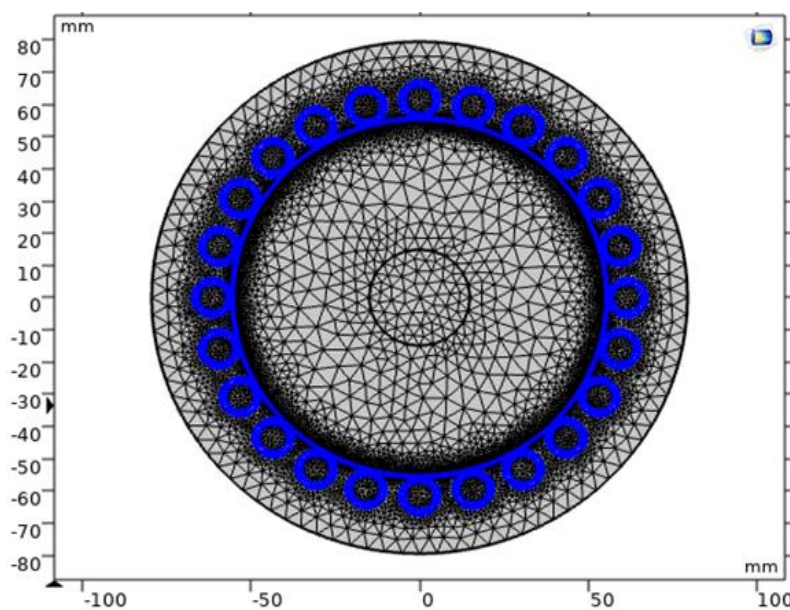


Figure 6. Mesh configuration of the six-phase induction motor

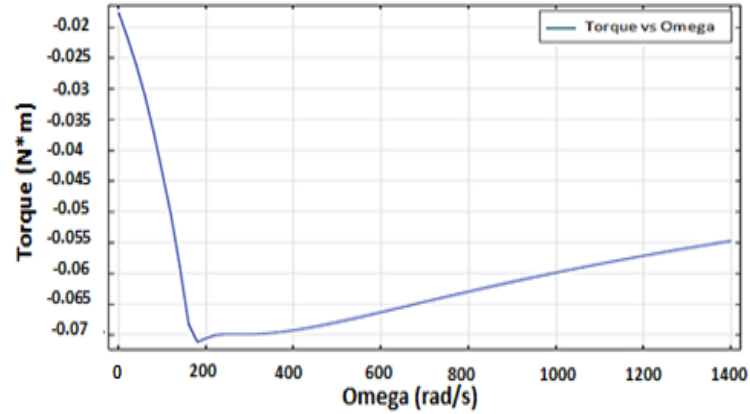


Figure 7. The 3-phase induction motor's torque and angular velocity (omega) relationship

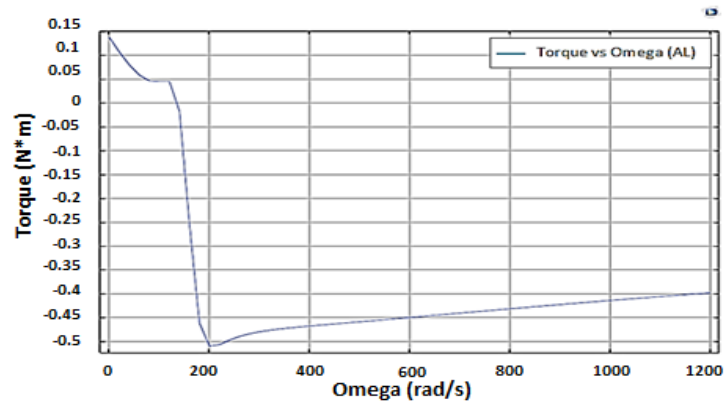


Figure 8. The 6-phase induction motor's torque and angular velocity relationship when the aluminum (AL) material

Figure 9 shows the relation between torque and angular velocity Ω when has been chosen the frequency domain analysis in a six-phase induction motor. Also, it observed the starting torque beginning is positive because of the increase in the flux density and ending in the negative value at the steady-state. The material has used in the rotor part is CI material. It is observed the starting up to 0.8 and steady-state approximately to equal -1.

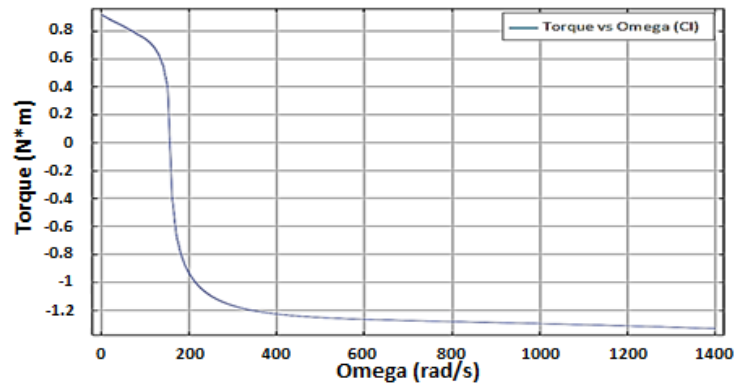


Figure 9. The relation between torque and angular velocity omega of the six-phase induction motor when the cast iron (CI) material

4. CONCLUSION

The scope of the paper is computer simulation help for the design of induction motors in their basic form useful to design adjustment. For the same design has a centered on two situations, first the MFD simulation three-phase and six-phase and the changing of the core materials of the rotor part for the induction motor. Second, changing of materials has been used with frequency domain in COMSOL program for the same design. The results showed the superior performance of the first situation for the six-phase MFD for time dependence and frequency domain when taken the FEM in considered. Also, the results have been shown in the second situation the positive effect of CI compared with AL on the performance in the relation between torque and angular velocity ω .

ACKNOWLEDGEMENTS

The authors would like to express their gratitude to the Northern Technical University of Iraq/Mosul Technical Institute for their aid in advancing this study.




REFERENCES

- [1] S. Bindu and V. V. Thomas, "Diagnoses of internal faults of three phase squirrel cage induction motor - A review," *2014 International Conference on Advances in Energy Conversion Technologies (ICAECT)*, 2014, pp. 48-54, doi: 10.1109/ICAECT.2014.6757060.
- [2] S. Manoharan, N. Devarajan, S. M. Deivasahayam, and G. Ranganathan, "Review on efficiency improvement in squirrel cage induction motor by using DCR technology," *Journal of Electrical Engineering*, vol. 60, no. 4, pp. 227-236, 2009.
- [3] Z. S. Hussain, A. J. Ali, A. A. Allu, and R. K. Antar, "Improvement of protection relay with a single phase auto reclosing mechanism based on artificial neural network," *International Journal of Power Electronics and Drive System (IJPEDS)*, vol. 11, no. 1, pp. 505-514, Mar. 2020, doi: 10.11591/ijpeds.v11.i1.pp505-514.
- [4] C. Sadarangani, "Electrical machines: design and analysis of induction and permanent magnet motors," *Division of Electrical Machines and Power Electronics*, 2006.
- [5] J. F. Gieras, C. Wang, and J. C. S. Lai, "Noise of polyphase electric motors," *Taylor & Francis*, 2006, doi: 10.1201/9781420027730.
- [6] K. R. Davey, "Analytic analysis of single- and three-phase induction motors," in *IEEE Transactions on Magnetics*, vol. 34, no. 5, pp. 3721-3727, Sep. 1998, doi: 10.1109/20.718534.
- [7] P. Venter, A. A. Jimoh and J. L. Munda, "Realization of a "3 & 6 phase," induction machine," *2012 XXth International Conference on Electrical Machines*, 2012, pp. 447-453, doi: 10.1109/ICEIMach.2012.6349907.
- [8] K. Rizwan, A. Iqbal, Sk. Moin, S. Moinuddin, and S. Payami, "Multi-phase alternative current machine winding design," *International Journal of Engineering, Science and Technology*, vol. 2, no. 10, pp. 79-86, 2010, doi: 10.4314/ijest.v2i10.64014.
- [9] R. O. C. Lyra and T. A. Lipo, "Torque density improvement in a six-phase induction motor with third harmonic current injection," in *IEEE Transactions on Industry Applications*, vol. 38, no. 5, pp. 1351-1360, Sep.-Oct. 2002, doi: 10.1109/TIA.2002.802938.
- [10] A. N. Hussain, A. J. Ali, and F. S. Ahmed, "Power quality improvement based on hybrid coordinated design of renewable energy sources for DC link channel DSTATCOM," *International Journal of Electrical and Computer Engineering (IJECE)*, vol. 10, no. 5, pp. 5108-5122, Oct. 2020, doi: 10.11591/ijece.v10i5.pp5108-5122.
- [11] M. Bose, A. Bhattacharjee, and Sudha, "Calculation of induction motor model parameters using finite element method," *International Journal of Soft Computing and Engineering (IJSCE)*, vol. 2, no. 3, pp. 41-43, Jul. 2012.
- [12] E. Schlemmer, "Finite element analysis of electrical machines used in two-frequency indirect temperature rise tests," *International Conference on Renewable Energies and Power Quality (ICREPQ'09)*, Apr. 2009.
- [13] M. Greconici, C. Koch and G. Madescu, "Advantages of FEM analysis in electrical machines optimization used in wind energy conversion systems," *2011 IEEE 3rd International Symposium on Exploitation of Renewable Energy Sources (EXPRES)*, 2011, pp. 91-94, doi: 10.1109/EXPRES.2011.5741798.
- [14] N. T. García, Y. A. G. Gómez, and F. E. H. Velasco, "Parameter estimation of three-phase linear induction motor by a DSP-based electric-drives system," *International Journal of Electrical and Computer Engineering (IJECE)*, vol. 10, no. 1, pp. 626-636, Feb. 2020, doi: 10.11591/ijece.v10i1.pp626-636.
- [15] J. A-K. Mohammed, S. R. Al-Sakini, and A. A. Hussein, "Assessment of disturbed voltage supply effects on steady-state performance of an induction motor," *International Journal of Electrical and Computer Engineering (IJECE)*, vol. 10, no. 3, pp. 2259-2270, 2020, doi: 10.11591/ijece.v10i3.pp2259-2270.
- [16] B. Somashekar, "Design of three phase induction motor using MATLAB programming," *International Journal on Recent and Innovation Trends in Computing and Communication*, vol. 3, no. 8, pp.5188-5193, Aug. 2015.
- [17] I. Bouneb and F. Kerrou, "Nanometric modelization of gas structure, multidimensional using COMSOL software," *International Journal of Electrical and Computer Engineering (IJECE)*, vol. 8, no. 4, pp. 2014-2020, Aug. 2018, doi: 10.11591/ijece.v8i4.pp2014-2020.
- [18] J. Güdelhöfer, R. Gottkehaskamp, and A. Hartmann, "Numerical calculation of the dynamic behavior of asynchronous motors with COMSOL multiphysics," *COMSOL Multiphysics Conference Milan 2012*, 2012.
- [19] Y. L. Karnavas and I. D. Chasiotis, "Influence of soft magnetic materials application to squirrel cage induction motor design and performance," *Engineering Journal*, vol. 21, no. 1, pp. 193-206, Jan. 2017, doi: 10.4186/ej.2017.21.1.193.
- [20] B. Ai, Y. Ai and L. Niu, "Study on the airgap flux density of the six-phase induction machine based on trapezoidal phase current waveform with CAD," *2010 International Forum on Information Technology and Applications*, 2010, pp. 343-346, doi: 10.1109/IFITA.2010.62.
- [21] Y. L. Ai, M. J. Kamper, Y. M. Wang and S. Y. Yuan, "Torque performance investigation of double three-phase motor using special current waveform," *The 4th International Power Electronics and Motion Control Conference, 2004. IPEMC 2004*, vol. 3, 2004, pp. 1673-1678.
- [22] S. Kocman, P. Pecinka, and T. Hruba, "Induction motor modeling using comsol multiphysics," *2016 17th International Scientific Conference on Electric Power Engineering (EPE)*, 2016, doi: 10.1109/EPE.2016.7521727.




- [23] R. Escarela-Perez, E. Melgoza and J. Alvarez-Ramirez, "Systematic coupling of multiple magnetic field systems and circuits using finite element and modified nodal analyses," in *IEEE Transactions on Magnetics*, vol. 47, no. 1, pp. 207-213, Jan. 2011, doi: 10.1109/TMAG.2010.2087387.
- [24] E. Levi, "Multiphase electric machines for variable-speed applications," in *IEEE Transactions on Industrial Electronics*, vol. 55, no. 5, pp. 1893-1909, May 2008, doi: 10.1109/TIE.2008.918488.
- [25] J. Martines, A. Belahcen, and A. Arkkio, "A 2D FEM model for transient and fault analysis of induction machines," *Przegląd Elektrotechniczny*, vol. 2012, no. 7b, pp. 157-160, 2449- 9544, 2012.
- [26] V. N. Savov, Zh. D. Georgiev, and E. S. Bogdanov, "Analysis of cage induction motor by means of the finite element method and coupled system of field circuit and motion equations," *Electrical Engineering*, vol. 80, no. 1, pp. 21-28, 1997, doi: 10.1007/BF01235666.
- [27] K. Yamazaki, "An efficient procedure to calculate equivalent circuit parameter of induction motor using 3-D nonlinear time-stepping finite-element method," in *IEEE Transactions on Magnetics*, vol. 38, no. 2, pp. 1281-1284, Mar. 2002, doi: 10.1109/20.996327.
- [28] E. B. Agamloh and A. Cavagnino, "High efficiency design of induction machines for industrial applications," *2013 IEEE Workshop on Electrical Machines Design, Control and Diagnosis (WEMDCD)*, 2013, pp. 33-46, doi: 10.1109/WEMDCD.2013.6525163.
- [29] V. Chandrasekaran, "Certain approaches in the design of induction machines for energy conservation," Ph.D. Dissertation, Faculty of Electrical Engineering, ANNA University, Feb. 25, 2014. [Online]. Available: <https://shodhganga.inflibnet.ac.in/handle/10603/16354>
- [30] D. T. Faeg, J. Raafat, and M. M. E. Ali, "Comparison of magnetic flux density for six-phase and three-phase induction motor using COMSOL multiphysics," *Journal of Zankoy Sulaimani*, pp. 1-10, 2019, doi: 10.17656/jzs.10752.
- [31] F. S. Ahmed and N. A. Al-jawady, "Control of prosthetic hand by using mechanomyography signals based on support-vector machine classifier," *Indonesian Journal of Electrical Engineering and Computer Science (IJECS)*, vol. 23, no. 2, pp. 1180-1187, Aug. 2021, doi: 10.11591/ijeecs.v23.i2.pp1180-1187.

BIOGRAPHIES OF AUTHORS






Firas Saaduldeen Ahmed    was born in Mosul, Nineveh, Iraq in 1984. He earned a bachelor's degree in electrical power engineering from Mosul's Technical Engineering College in 2007 and a master's degree in the same area from Bagdad's Electrical Engineering Technical College in 2020. From 2021, are taught power electronics, digital, single and, three-phase machine, and Programmable logical control (PLC) at Mosul Technical Institute/Northern Technical University of Iraq. He has five papers in a field electrical power system and computer engineering (modern algorithms). He can be contacted at email: firmas_saad@ntu.edu.iq



Zozan Saadallah Hussain    was born in Mosul, Nineveh, Iraq in 1986. She earned a B.S degree in electrical power engineering from the Technical Engineering College Mosul in 2007, and a master's degree in the same field and same department, Iraq in 2010. From 2010, are taught power electronics, digital, single and, three-phase machine, and Programmable logical control (PLC) at Mosul Technical Institute/Northern Technical University of Iraq. He has four papers in a field electrical power system and computer engineering (modern algorithms). She can be contacted at email: zozan.hussain@gmail.com



Truska Khalid Mohammed Salih    was born in Kirkuk, Iraq in 1986. She received a B.S degree from the University of Sulaimanya in 2009, and a Master degree from the University of Salahadeen in 2019. She started teaching A.C and D.C Electrical Circuit at Erbil technology college from 2020. She has one research in electrical field. She can be contacted at email: truska.muhamad@epu.edu.iq